insulin stimulation phosphorylation of Tyr 1162-1163 precedes receptor aggregation and (ii) no additional information which is mediated by the insulin receptor (related to tyrosine kinase activation) seems to be necessary for the propagation of the postreceptor signal leading to glycogen synthesis, once the physical receptor aggregation is achieved.

ACKNOWLEDGMENTS

We are very grateful to C. Filloux and C. Auzan for skillful technical help and X. Morinay and F. Aguilla for illustrations. We also thank G. W. G. Sharp for carefully reading the manuscript and for fruitful discussions.

REFERENCES

Braun, S., Raymond, W. E., & Racker, E. (1984) *J. Biol. Chem. 259*, 2051-2054.

Chou, C. K., Dull, T. J., Russel, D. S., Gherzi, R., Lebwolh, D., Ullrich, A., & Rosen, O. M. (1987) *J. Biol. Chem. 262*, 1842-1847.

Debant, A., Clauser, E., Ponzio, G., Filloux, C., Auzan, C., Contreres, J. O., & Rossi, B. (1988) *Proc. Natl. Acad. Sci. U.S.A.* (in press).

Ellis, L., Clauser, E., Morgan, D. O., Edery, M., Roth, R. A., & Rutter, W. J. (1986) *Cell 45*, 721-732.

Forsayeth, J. R., Caro, J. F., Sinha, M. K., Maddux, B. A., & Goldfine, I. R. (1987) *Proc. Natl. Acad. Sci. U.S.A. 84*, 3448-3451.

Gherzi, R., Russel, D. S., Taylor, S. I., & Rosen, O. M. (1987) *J. Biol. Chem. 35*, 16900-16905.

Kahn, C. R., Baird, K. L., Jarret, B. D., & Flier, J. S. (1978) *Proc. Natl. Acad. Sci. U.S.A. 73*, 4209-4213.

O'Brien, R. M., Soos, M. A., & Siddle, K. (1987) *EMBO J. 6*, 4003-4010.

Ponzio, G., Dolais-Kitabgi, J., Louvard, D., Gautier, N., & Rossi, B. (1987) *EMBO J. 6*, 333-340.

Schreiber, A. B., Libermann, J. A., Lax, I., Yarden, Y., & Schlessinger, J. (1983) *J. Biol. Chem. 258*, 846-853.

Simpson, I. A., & Hedo, J. A. (1984) *Science 223*, 1301-1303.

Articles

Cholesterol Modifies the Short-Range Repulsive Interactions between Phosphatidylcholine Membranes†

Thomas J. McIntosh,*,‡ Alan D. Magid,‡ and Sidney A. Simon§

Departments of Cell Biology, Neurobiology, and Anesthesiology, Duke University Medical Center, Durham, North Carolina 27710

Received May 23, 1988; Revised Manuscript Received July 13, 1988

ABSTRACT: Pressure versus distance relationships have been obtained for egg phosphatidylcholine bilayers containing a range of cholesterol concentrations. Water was removed from between adjacent bilayers by the application of osmotic pressures in the range of 0.4–2600 atm (4×10^5–2.6×10^9 dyn/cm^2), and the distance between adjacent bilayers was obtained by Fourier analysis of X-ray diffraction data. For applied pressures up to about 50 atm and bilayer surface separations of 15–5 Å, the incorporation of up to equimolar cholesterol has little influence on plots of pressure versus bilayer separation. However, for the higher applied pressures, cholesterol reduces the interbilayer separation distance by an amount that depends on the cholesterol concentration in the bilayer. For example, the incorporation of equimolar cholesterol reduces the distance between bilayers by as much as 6 Å at an applied pressure of 2600 atm. At this applied pressure, electron density profiles show that the high-density head-group peaks from apposing bilayers have merged. This indicates that equimolar concentrations of cholesterol spread the lipid molecules apart in the plane of the bilayer enough to allow the phosphatidylcholine head groups from apposing bilayers to interpenetrate as the bilayers are squeezed together. All of these X-ray and pressure–distance data indicate that, by reducing the volume fraction of phospholipid head groups, cholesterol markedly reduces the steric repulsion between apposing bilayers but has a much smaller effect on the sum of the longer ranged repulsive hydration and fluctuation pressures. Increasing concentrations of cholesterol monotonically increase the dipole potential of egg phosphatidylcholine monolayers, from 415 mV with no cholesterol to 493 mV with equimolar cholesterol. These dipole measurements predict that cholesterol should increase slightly the magnitude of the hydration pressure, in qualitative agreement with the X-ray results. These observations are pertinent to cholesterol's role in vesicle adhesion and fusion and also imply that cholesterol can alter the membrane binding and permeability of ions and certain drugs and metabolites.

The close approach of uncharged bilayer membranes is thought to be resisted by three principal nonspecific repulsive interactions. The first of these, commonly called the solvation or hydration pressure, P_h, arises from the polarization of water molecules by the zwitterionic lipid head groups (Marcelja & Radic, 1976; LeNeveu et al., 1976, 1977; Israelachvili & Pashley, 1983). It has been found empirically that $P_h = P_0 \exp(-d_f/\lambda)$, where d_f is the distance between bilayers and the decay length λ is on the order of 1–3 Å (LeNeveu et al., 1977; Parsegian et al., 1979; Lis et al., 1982; McIntosh & Simon,

† Supported by NIH Grant GM 27278.

‡ Department of Cell Biology.

§ Departments of Neurobiology and Anesthesiology.

0006-2960/89/0428-0017$01.50/0

1986a). The hydration pressure is considered to be the dominant repulsive pressure in the range of d_f = 5–15 Å (LeNeveu et al., 1977; Parsegian et al., 1979). The second repulsive pressure demonstrated between bilayers, which has been called the undulation or fluctuation pressure, P_f, arises from thermally induced fluctuations in the bilayer surface (Harbich & Helfrich, 1984; Evans & Parsegian, 1986; Evans & Needham, 1987). A recent theoretical model (Evans & Parsegian, 1986; Evans & Needham, 1987) predicts that, for neutral liquid-crystalline bilayers, P_f enhances hydration repulsion for large bilayer separations (d_f > 15 Å). The third repulsive interaction is due to steric hindrance between apposing lipid head groups which extend from the hydrocarbon–water interface into the fluid space between bilayers. Recently, it has been shown for phosphatidylcholine (PC) bilayers that steric hindrance forms the major repulsive barrier between adjacent bilayers for fluid thicknesses of less than about 5 Å (McIntosh et al., 1987).

It is of interest to understand how these repulsive interactions are modified by the presence of cholesterol in the bilayer. Cholesterol is an important component of many plasma membranes and has been shown to have significant effects on membrane structure (Franks, 1976; Worcester & Franks, 1976; McIntosh, 1978), fluidity (Darke et al., 1972; Oldfield & Chapman, 1972; Stockton & Smith, 1976), compressibility (Evans & Needham, 1987), and permeability to electrolytes and nonelectrolytes (Szabo, 1974, 1976; Cohen, 1975). Cholesterol might also be expected to modify the repulsive pressures between adjacent bilayers for several reasons. First, in terms of the hydration pressure, it is known that cholesterol modifies the hydration of bilayers (Taylor et al., 1977; Jendrasiak & Hasty, 1974; Ter-Minassian-Saraga & Madelmont, 1982), the depth of water penetration into bilayers (Simon et al., 1982), and the association of adjacent PC[1] bilayers (Stamatatos & Silvius, 1987). Cholesterol has also been shown to be a major factor in the formation of atherosclerotic plaques (Small & Shipley, 1974). In addition, by virtue of its ability to separate PC head groups in the plane of the bilayer, cholesterol might be expected to modify both hydration and steric interactions between apposing membranes; for PC bilayers the magnitudes of both of these pressures have been shown to depend on the density of zwitterionic lipid head groups at the water–bilayer interface (McIntosh et al., 1987; Simon et al., 1988). In terms of the fluctuation pressure, the addition of cholesterol would be expected to decrease thermally induced undulations, since it stiffens the bilayer, that is, it increases the bilayer bending modulus (Evans & Needham, 1987). Finally, the addition of cholesterol to PC bilayers should modify the van der Waals attraction, both by increasing the electron density and polarizability of the bilayer hydrocarbon region (Nir, 1976) and by changing the contribution of the polar head-group region (Attard et al., 1988).

The present study was undertaken to determine quantitatively the effects that cholesterol has on the repulsive interactions between membrane surfaces. By the use of X-ray diffraction analysis of bilayers brought together by applied osmotic pressures, we have measured pressure versus fluid separation for egg phosphatidylcholine bilayers containing a range of cholesterol concentrations.

Materials and Methods

Egg phosphatidylcholine (EPC) was obtained from Avanti Polar Lipids, Inc., and cholesterol (99+%) was obtained from either Avanti Polar Lipids or Sigma Chemical Co. Both lipids were used without further purification. Poly(vinylpyrrolidone) (PVP) with an average molecular weight of 40 000 was obtained from Sigma Chemical Co. Triply distilled water was used to make PVP–water solutions in the range of 0–60% w/w.

Osmotic pressure was applied to unoriented lipid suspensions by the "osmotic stress" procedures of Parsegian, Rand, and colleagues (LeNeveu et al., 1976; Parsegian et al., 1979, 1986). In brief, EPC–cholesterol mixtures were rotary evaporated from chloroform, and an excess amount (usually 70% by weight) of the appropriate PVP solution was added. The suspensions were incubated under nitrogen for several hours with periodic vortexing. An excess fluid phase was visible either by direct observation or by light microscopy. Because PVP is too large to enter between the lipid multilayers, it competes for water with the lipid and therefore compresses the lamellar lattice (LeNeveu et al., 1976; Parsegian et al., 1979). Osmotic pressures of the PVP solutions were calculated from the virial coefficients obtained by Vink (1971). These extrapolated pressures are in close agreement with values measured by Parsegian et al. (1986) and by us (unpublished results). The lipid–PVP suspensions were sealed in quartz glass X-ray capillary tubes and mounted in a point collimation X-ray camera.

Vapor pressures were applied to oriented multilayers by published procedures (Parsegian et al., 1979; McIntosh et al., 1987). The multilayers were formed by placing a small drop of EPC/cholesterol/chloroform solution on a flat strip of aluminum foil and evaporating the chloroform. The aluminum foil substrate was given a convex curvature by bending around a Pasteur pipet. The specimen was mounted in a controlled humidity chamber on a line-focused single-mirror X-ray camera, so that the X-ray beam was oriented at a grazing angle relative to the oriented multilayers. Relative humidity was controlled in the chamber by means of a cup of a saturated salt solution. To speed equilibration, a gentle stream of nitrogen gas was passed through a flask of the saturated salt solution and then through the chamber. The ratios of the vapor pressure (p) of various salt solutions to the vapor pressure of pure water (p_0) have been measured (O'Brien, 1948; Weast, 1984). The following saturated salt solutions were used to obtain the relative vapor pressure (p/p_0) indicated in parentheses: $CuSO_4$ (0.98), Na_2SO_4 (0.93), KCl (0.87), NH_4Cl (0.80), $NaNO_2$ (0.66), $Na_2Cr_2O_7 \cdot 2H_2O$ (0.52), $CaCl_2$ (0.32), $KC_2H_3O_2$ (0.20), and LiCl (0.15). The applied vapor pressure is given by

$$P = -(RT/V_w) \ln (p/p_0) \quad (1)$$

where R is the molar gas constant, T is the temperature, and V_w is the molar volume of water.

For both oriented multilayers and unoriented lipid–PVP suspensions X-ray diffraction patterns were recorded on a stack of three or four sheets of Kodak DEF 5 X-ray film. Films were processed by standard techniques and densitometered with a Joyce-Loebl Model MKIIIC microdensitometer. For the unoriented specimens, the densitometer trace was taken in a radial direction from the center of the film, whereas for the oriented specimens the trace was taken through the center of each reflection. After background subtraction, integrated intensities, $I(h)$, were obtained for each order h by measuring the area under each diffraction peak. For unoriented patterns the structure amplitude $F(h)$ was set equal to $[h^2I(h)]^{1/2}$ (Herbette et al., 1977; Blaurock & Worthington, 1966). For the oriented, line-focused patterns, there was no detectable arcing of the reflections, which were of uniform height. In this case, intensities were corrected by a single factor of h (the

[1] Abbreviations: PC, phosphatidylcholine; EPC, egg phosphatidylcholine; DMPC, dimyristoylphosphatidylcholine; DPPC, dipalmitoylphosphatidylcholine; SOPC, 1-stearoyl-2-oleoylphosphatidylcholine.

Lorentz correction factor) due to the cylindrical curvature of the multilayers (Herbette et al., 1977; Blaurock & Worthington, 1966), so that $F(h) = [hI(h)]^{1/2}$. The validity of this correction factor was demonstrated by the observation that structure amplitudes for the oriented specimens at high vapor pressures (0.98 and 0.93) fell on the same continuous transform as obtained from the unoriented suspensions at equivalent osmotic pressures [see McIntosh and Simon (1986a) and Figure 2 below]. In addition, electron density profiles for these humidities are very similar to those obtained at equivalent osmotic pressures (McIntosh et al., 1987). Electron density profiles were calculated by

$$\rho(x) = (2/d)\sum_h \exp[i\phi(h)]F(h) \cos(2\pi hx/d)$$

where d is the lamellar repeat period and $\phi(h)$ is the phase angle, either 0 or π for each order h. Published phase angles were used for bilayers of EPC (Torbet & Wilkins, 1976; McIntosh & Simon, 1986a) and EPC/cholesterol (Franks, 1976).

Continuous transforms were calculated from the structure factors [$=\exp(i\phi)F(h)$] for each data set by the use of the sampling theorem (Shannon, 1949) as previously described (McIntosh & Simon, 1986a). The value of the structure factor at the origin of reciprocal space was estimated by the procedure of King and Worthington (1971).

For dipole potential measurements, the appropriate molar ratios of EPC and cholesterol were codissolved in chloroform (25 mg/mL). Monolayers were formed by spreading 10 μL of the lipid solution onto 1 mM KCl in a Teflon trough with a surface area of about 30 cm^2. The KCl was roasted at 600 °C, the water was triply distilled, and the subphase was vacuum aspirated before the monolayer was spread to ensure that the surface was free of surface-active impurities. The trough was emptied and thoroughly cleaned between runs. All measurements were made at a temperature of 21 ± 2 °C. Under these conditions it has previously been shown that the packing of the molecules in the monolayer is approximately the same as it is in a bilayer (MacDonald & Simon, 1987). The dipole potential was measured between a Ag/AgCl electrode in the subphase and a polonium electrode in the air which were connected to a Keithley electrometer, Model 602. The reported values of the dipole potential represent the difference in the potential of the subphase surface in the presence and absence of the monolayer.

Results

For both oriented and unoriented EPC/cholesterol specimens, the diffraction patterns consisted of a series of low-angle reflections, which indexed as orders of a lamellar repeat period, and a broad wide-angle band with a spacing of about 4.5 Å. These patterns are typical of bilayers in the liquid-crystalline or L_α phase (Tardieu et al., 1973). The repeat periods at full hydration were found to be 63.2, 65.9, 66.3, and 65.9 Å, for egg PC bilayers containing 0.0, 0.2, 0.33, and 0.5 mole fraction cholesterol, respectively. The following range of repeat periods were obtained for applied pressures of 4.3×10^5 dyn/cm^2 (with 10% PVP) to 2.6×10^9 dyn/cm^2 (with 0.15 relative vapor pressure). For 0.2 mole fraction cholesterol d ranged from 62.0 to 50.8 Å, for 0.33 mole fraction cholesterol d ranged from 62.5 to 47.2 Å, and for 0.5 mole fraction cholesterol d ranged from 63.6 to 44.7 Å. Previously we had found for similar conditions that the range of d for EPC bilayers was 59.2–49.9 Å (McIntosh & Simon, 1986a). The natural logarithm of applied pressure (ln P) is plotted versus repeat period for EPC and EPC containing 0.5 mole fraction cholesterol in Figure

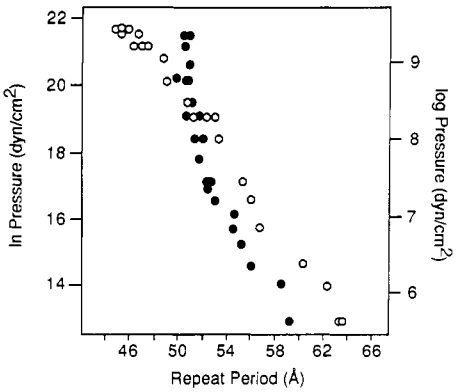

FIGURE 1: Natural logarithm (left-hand scale) and common (base 10) logarithm (right-hand scale) of applied pressure plotted versus lamellar repeat period for EPC bilayers containing 0 (solid circles) and 0.5 mole fraction cholesterol (open circles).

1. For the low-pressure range (ln P less than 18) the repeat periods for the cholesterol-containing specimens are about 3 Å greater than for EPC multilayers at each applied pressure. However, as shown previously (McIntosh et al., 1987), the ln P versus d curve for EPC has a distinct upward break at ln P = 18, whereas there is no such break in the equimolar EPC/cholesterol data. Thus, the plots of ln P versus d for the two data sets intersect at ln $P \simeq 18.5$, and for the highest applied pressure (ln P = 21.7), the repeat period for EPC/cholesterol is 5–6 Å less than for EPC.

To obtain estimates for the bilayer thickness (d_b) and the separation between bilayer surfaces (d_f) for each pressure experiment, the following structural analysis was performed. Panels A, B, and C of Figure 2 show structure factors (circles) for each experiment plotted versus reciprocal space coordinate for EPC containing 0.5, 0.33, and 0.2 mole fraction cholesterol, respectively. Previously we have published similar plots for EPC multilayers (McIntosh & Simon, 1986a). In each plot in Figure 2, the solid line represents the mean value of all transforms calculated from each data set, and the stippled lines show plus and minus 1 standard deviation from the mean. For each cholesterol concentration the structure factors fall fairly close to the mean transform. This indicates that for each cholesterol concentration the width of the bilayer remains constant (to within 1–2 Å) over the range of applied pressures (McIntosh & Simon, 1986a). Note, however, that the shape of the transform depends on the amount of cholesterol in the bilayer, indicating that the structure of the bilayers is modified by the incorporation of cholesterol.

Figure 3 shows electron density profiles for EPC bilayers containing 0, 0.33, and 0.5 mole fraction cholesterol at a relative vapor pressure of 0.98. For each profile, the geometric center of the bilayer is at the origin (0 Å). The low-density troughs in the center of each profile correspond to the localization of lipid terminal methyl groups, and the highest density peaks, located at about ±19 Å for 0 mole fraction cholesterol and at about ±20 Å for 0.33 and 0.5 mole fraction cholesterol, correspond to the PC head groups. The medium-density regions between the terminal methyl trough and the head-group peaks represent the methylene chain region of the bilayer, and the medium-density regions at the outer edges of each profile correspond to the fluid spaces between adjacent bilayers. These profiles indicate that the incorporation of cholesterol into EPC multilayers increases the distance across the bilayer between the head-group peaks and raises the electron density of the methylene chain region relative to the terminal methyl trough. These effects have previously been noted and can be explained by the localization

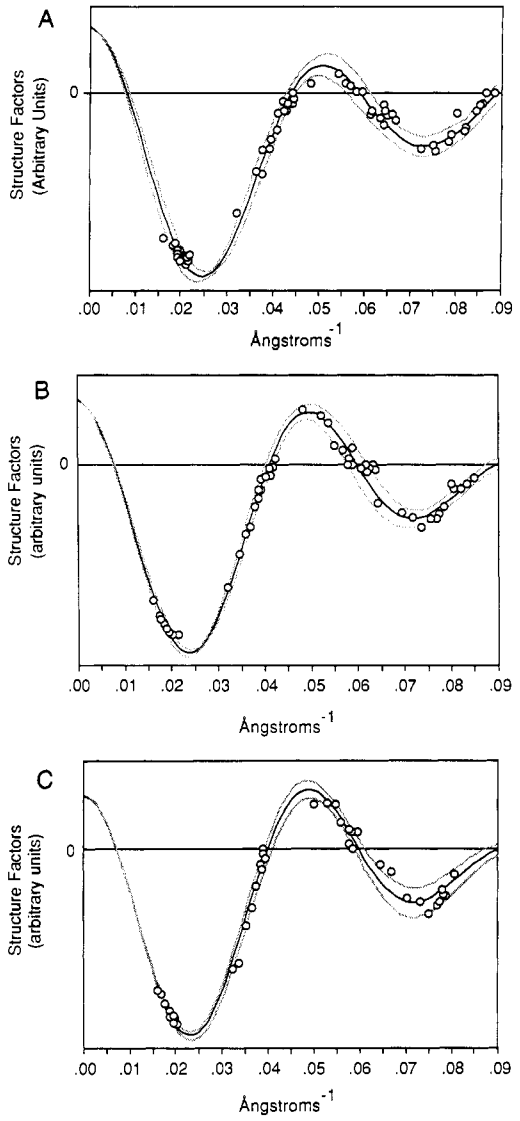

FIGURE 2: Structure factors and continuous transforms plotted versus reciprocal space coordinate for EPC bilayers containing (A) 0.5 mole fraction cholesterol, (B) 0.33 mole fraction cholesterol, and (C) 0.2 mole fraction cholesterol. For each graph the open circles represent the structure factors for all pressure experiments, the solid lines represent the mean values of the continuous transforms calculated with each data set, and the dashed curves show ±1 standard deviation from the mean. In this figure, three diffraction orders are used for repeat periods less than 46.5 Å, four orders are used for 46.5 Å < d < 60 Å, and five orders are used for d > 60Å.

of cholesterol in the hydrocarbon region of the bilayer, adjacent to the PC head groups (McIntosh, 1978).

Panels A and B of Figure 4 show electron density profiles over a range of applied pressures for EPC containing 0.2 and 0.5 mole fraction cholesterol, respectively. Notice that the distance between bilayers decreases with increasing applied pressure. However, the distance between head-group peaks across the bilayer remains essentially constant for this entire range of applied pressures. The distance between head-group peaks across the bilayers is 40.0 ± 0.4 Å (mean ± standard deviation, N = 10 experiments) for 0.2 mole fraction cholesterol, 40.2 ± 0.4 Å (N = 16) for 0.33 mole fraction cholesterol, and 39.7 ± 0.7 Å (N = 12) for 0.5 mole fraction cholesterol. (As discussed in the next paragraph, distances between head-group peaks could not be obtained for 0.5 mole fraction cholesterol at the higher applied pressures.) These values can be compared to the corresponding value of 37.8 ± 0.8 Å for EPC for the pressure range 12 < ln P < 18

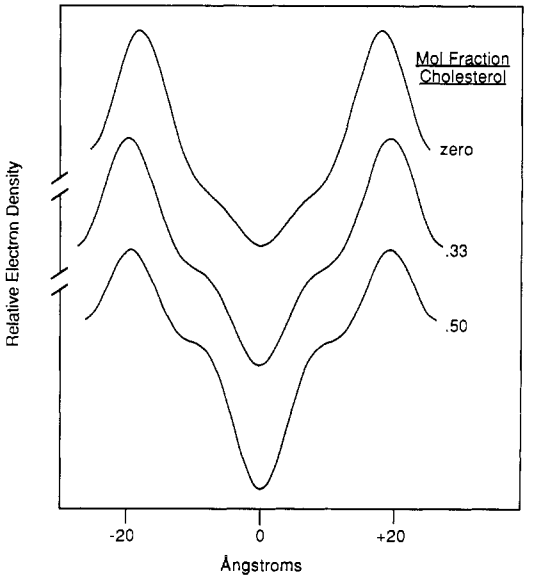

FIGURE 3: Electron density profiles for EPC bilayers containing 0, 0.33, and 0.5 mole fraction cholesterol at a relative vapor pressure of 0.98. All profiles are on an arbitrary electron density scale.

(McIntosh & Simon, 1986a). For pressures higher than ln P = 18, the separation of head-group peaks in profiles of EPC increases, reaching a maximum of about 40 Å at ln P = 21.5 (McIntosh et al., 1987). Thus, EPC/cholesterol bilayers are 2–3 Å wider than EPC bilayers at low applied pressures (ln P < 18) but have approximately the same width as EPC bilayers at the highest applied pressure (ln P = 21.5).

The major difference among the profiles shown in Figure 4 occurs at the higher applied pressures. For 0.2 mole fraction cholesterol the fluid space between adjacent bilayers is large enough at all applied pressures that the apposing head-group peaks are clearly resolved. This was also the case for EPC bilayers (McIntosh et al., 1987) and for 0.33 mole fraction cholesterol (data not shown). However, for 0.5 mole fraction cholesterol at the higher applied pressures (ln P > 21) the fluid separation is so small that the head-group peaks from apposing bilayers have merged, so that the peaks from apposing bilayers are not resolved. The resolution of these profiles ($d/2h_{max}$) is about 5.7 Å, implying that at the highest applied pressures the centers of the high-density peaks are within 6 Å of each other. The electron density profiles of Lesslauer et al. (1972) for dipalmitoylphosphatidylcholine (DPPC) bilayers and of Franks and Lieb (1979) for dimyristoylphosphatidylcholine (DMPC) bilayers with cholesterol show that, at this resolution, the high-density peaks in the profiles fall near the center of the PC head group, between the phosphate moiety and the glycerol backbone. If in these egg PC/cholesterol bilayers the PC head groups were oriented approximately parallel to the plane of the membrane, as they are in crystals (Pearson & Pascher, 1979), the high electron density peak would be about 5 Å from the edge of the bilayer (McIntosh & Simon, 1986a; McIntosh et al., (1987). Since the high-density peaks are separated by less than 6 Å for the profiles where the peaks have merged (Figure 4A), this implies for these bilayers that the head groups from apposing bilayers have interpenetrated by about 4 Å. If the head groups were oriented, on average, so that they extended out from the plane of the bilayer into the fluid phase, then the depth of interpenetration would be larger than 4 Å.

The electron density profiles can be used to estimate the distance between adjacent bilayers at each applied pressure. As noted previously (McIntosh et al., 1987), the definition of

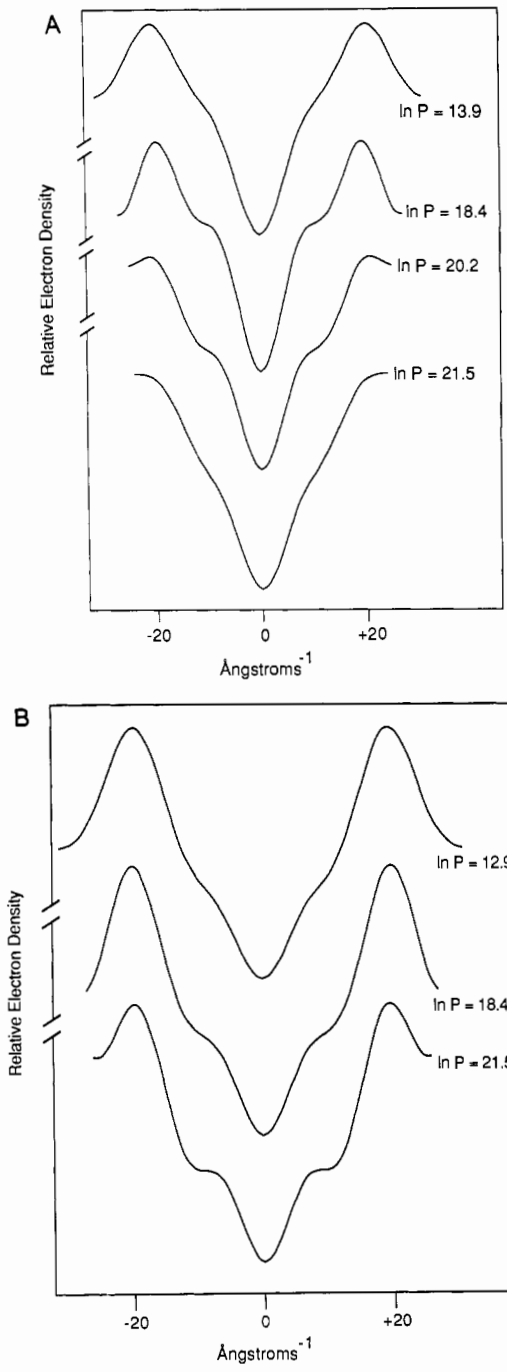

FIGURE 4: Electron density profiles of EPC bilayers containing (A) 0.5 mole fraction cholesterol and (B) 0.2 mole fraction cholesterol for a range of applied pressures.

fluid thickness is somewhat arbitrary for lipids with zwitterionic head groups for several reasons: (1) the bilayer surface is not molecularly smooth, (2) the lipid head groups are mobile (Hauser et al., 1981), and (3) water penetrates into the lipid head-group region (Worcester & Franks, 1976; Simon et al., 1982). As we have done previously (McIntosh & Simon, 1986a; McIntosh et al., 1987), we operationally defined the bilayer width as the total thickness of the bilayer assuming that the head-group conformation is the same as it is in single crystals of DMPC (Pearson & Pascher, 1979). That is, in this definition we assumed that the phosphocholine group is, on average, oriented approximately parallel to the bilayer plane, so that the edge of the bilayer lies about 5 Å outward from the center of the high-density peaks in the electron density profiles. Thus, for each applied pressure, d_b was set equal to

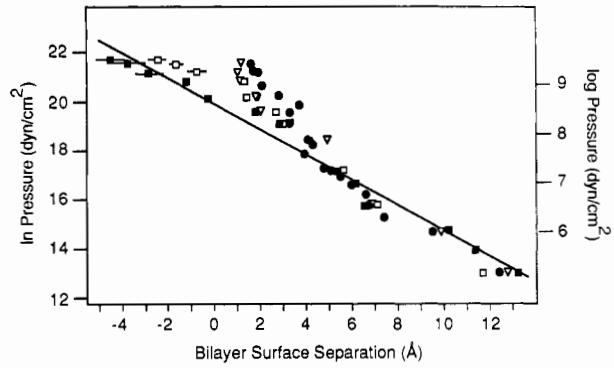

FIGURE 5: Natural logarithm (left-hand scale) and common logarithm (right-hand scale) of applied pressure plotted versus the separation between adjacent bilayer surfaces (d_f) estimated from electron density profiles for EPC bilayers containing 0 (●), 0.2 (▽), 0.33 (□), and 0.5 (■) mole fraction cholesterol. The solid line is a linear least-squares fit to the equimolar EPC/cholesterol data. For EPC containing 0.33 and 0.5 mole fraction cholesterol, the experiments at the three highest pressures were performed two or three times. The mean values for $d_f \pm 1$ standard deviation (horizontal lines) are shown for these experiments.

the distance between head-group peaks in the electron density profiles plus 10 Å (McIntosh & Simon, 1986a; McIntosh et al., 1987). For the case of EPC with 0.5 mole fraction cholesterol at high applied pressures, where the individual head-group peaks were not resolved, the average value of head-group peak separation (39.7 Å) from the other pressure experiments was used in this calculation (see above). This procedure was justified by the observation that the structure factors for these high-pressure experiments fell on the same continuous transform (Figure 2A) as for the lower pressure experiments, indicating that the bilayer thickness remained approximately constant for all applied pressures. The distance between bilayer surfaces, d_f, was then obtained from $d_f = d - d_b$. Note that, with these definitions for d_b and d_f, negative values of d_f correspond to interpenetration of polar head groups from apposing bilayers.

Figure 5 shows ln P plotted versus d_f for EPC bilayers containing 0, 0.2, 0.33, and 0.5 mole fraction cholesterol. The solid line corresponds to a linear least-squares fit to the equimolar EPC/cholesterol data, with a decay length of 1.9 Å. For ln $P < 17.5$, the data points at all cholesterol concentrations (from 0 to 0.5 mole fraction) fall quite close to this line. The results in this pressure range for equimolar EPC/cholesterol are in fairly close agreement with the results of Lis et al. (1982), who found for this system for this pressure range an exponential decay with a decay length of 1.4 Å. However, for $17.5 <$ ln $P < 20$ the data points for all cholesterol concentrations fall above the solid line. For ln $P > 20$, the values of d_f for the different concentrations of cholesterol diverge, so that at the highest applied pressure the fluid separation is about 6 Å less for EPC containing 0.5 mole fraction cholesterol than for EPC bilayers. For these highest applied pressures, values of d_f for bilayers containing 0.2 mole fraction cholesterol appear very similar to those for EPC bilayers, whereas d_f values for bilayers with 0.33 mole fraction cholesterol are intermediate between the extreme cases of 0.5 and 0 mole fraction cholesterol (Figure 5).

The magnitude of P_h has been shown to be proportional to the square of the dipole potential (Simon et al., 1988). Therefore we measured the dipole potential for EPC monolayers as a function of cholesterol concentration. The dipole potential was 415 ± 13 mV ($N = 3$ experiments) for EPC monolayers and 446 ± 15 mV ($N = 4$), 463 ± 6 mV ($N = 3$), and 493 ± 13 mV ($N = 3$) for EPC monolayers containing

0.2, 0.33, and 0.5 mole fraction cholesterol, respectively.

Discussion

The results presented in this paper can be used to obtain information on how the incorporation of cholesterol modifies each of the three repulsive pressures—steric, hydration, and fluctuation—which are thought to act between the surfaces of PC bilayers.

First let us consider cholesterol's effects on steric pressure. At an applied pressure of about 4×10^7 dyn/cm^2 ($\ln P = 17.5$), the experimental data points for EPC and EPC/cholesterol deviate upward for the solid curve in Figure 5. For EPC, this upward deviation, or increased resistance to compression, has been explained (McIntosh et al., 1987) in terms of steric repulsion between the mobile PC head groups which can extend 2–3 Å into the fluid space between bilayers. As would be predicted from our previous analysis (McIntosh et al., 1987), the extent of this upward deviation, particularly at higher applied pressures, depends on the surface density (or volume fraction) of EPC head groups in the plane of the bilayer. For instance, plots of $\ln P$ versus d_f (Figure 5) are very similar at high pressures for EPC bilayers containing 0 and 0.2 mole fraction cholesterol. That is, when pressures greater than 4×10^7 dyn/cm^2 ($\ln P > 17.5$) are applied, the fluid space between bilayers decreases only slightly due to the steric hindrance between apposing EPC head groups. However, for EPC containing 0.5 mole fraction cholesterol, there is a much larger decrease in d_f as the applied pressure is increased (Figure 5). In fact, the separation between bilayers is about 6 Å smaller for equimolar EPC/cholesterol bilayers than for EPC bilayers at the highest applied pressures. In addition, the electron density profiles presented in Figure 4A show that at high applied pressure the bilayers are so close that head groups from apposing bilayers have interpenetrated. For EPC bilayers containing 0.33 mole fraction cholesterol, the data points fall in between the extreme cases of 0 and 0.5 mole fraction cholesterol, indicating that the magnitude of steric repulsion depends on the amount of cholesterol in the bilayer.

These observations can be explained in terms of a simple model in which cholesterol spreads the EPC molecules apart in the plane of each bilayer, reducing the volume fraction of PC head groups at the interface, thereby decreasing steric repulsion between adjacent bilayers. For equimolar EPC/cholesterol bilayers the EPC molecules are evidently spread far enough apart that head groups from apposing bilayers can interpenetrate. The following calculations show that equimolar cholesterol can indeed increase the area per PC head group enough to allow interpenetration of apposing head groups. At a water content of 35% (which is near full hydration) Lecuyer and Dervichian (1969) used X-ray diffraction data to calculate the mean area per lipid molecule to be 64 Å^2 for EPC and 44 Å^2 for EPC with 0.5 mole fraction cholesterol. These calculations indicate that the area per EPC head group at the bilayer–water interface increases from about 64 to 88 Å^2 with the incorporation of equimolar cholesterol. Using similar techniques, Lis et al. (1982) obtained a somewhat higher value of 96 Å^2 for the area per PC head group in equimolar EPC/cholesterol bilayers at full hydration. The minimum area needed per PC head group in the bilayer plane can be equated to the measured area per molecule in the gel ($L_{\beta'}$) phase of DPPC. That is, in the $L_{\beta'}$ phase the area per molecule is determined primarily by the effective area occupied by each DPPC head group at the interface, since the lipid head group has a larger excluded area in the plane of the bilayer than do the gel-phase hydrocarbon chains (McIntosh, 1980). The minimum area per DPPC molecule measured by Tardieu et al. (1973) is 42.7 Å^2, which we take to be the excluded area per PC head group at the interface. Since this is less than half the area per EPC head group in bilayers composed of equimolar EPC and cholesterol, we conclude that the incorporation of 0.5 mole fraction cholesterol increases the area per EPC head group enough to allow the interpenetration of EPC head groups from apposing bilayers. Similar calculations show that the incorporation of 0.33 mole fraction cholesterol does not increase the area enough to allow complete interpenetration of polar groups. Thus, for the higher pressures ($\ln P > 20$), the values of d_f are larger for bilayers containing 0.33 mole fraction cholesterol than for bilayers containing equimolar cholesterol (Figure 5).

Thus, when high pressures ($\ln P > 18$) are applied to equimolar EPC/cholesterol bilayers, the head groups can slide by each other and cause a reduction in d_f of about 6 Å beyond what is observed with EPC bilayers. That is, it appears that high concentrations of cholesterol can effectively reduce the steric hindrance between apposing bilayers by reducing the density of PC head groups in the plane of each bilayer.

Next, consider the data for applied pressures less than 2.5×10^7 dyn/cm^2 ($\ln P < 17$). For these applied pressures steric repulsion between apposing bilayers is negligible (McIntosh et al., 1987), so that hydration and fluctuation pressures should be the dominant repulsive interactions. For $\ln P < 17$, plots of $\ln P$ versus fluid layer thickness are quite similar for EPC with 0, 0.2, 0.33, and 0.5 mole fraction cholesterol (Figure 5). This implies that the total pressure, P_t, which includes the contributions of hydration pressure (P_h), fluctuation pressure (P_f), and the attractive van der Waals pressure (P_V), is nearly the same for all cholesterol concentrations for this range of applied pressure. In support of this conclusion is the observation that the equilibrium fluid separation (the bilayer separation in the absence of applied pressure) is nearly the same for EPC and EPC/cholesterol bilayers. That is, the incorporation of from 0.2 to 0.5 mole fraction cholesterol causes a parallel increase of 2 to 3 Å in both the lamellar repeat period and the distance between head-group peaks across the bilayer in electron density profiles (Figure 3). This means that the incorporation of cholesterol does not appreciably change (to within 1 or 2 Å) the equilibrium water thickness between EPC bilayers, which is determined by a balance between P_v and the sum of P_h and P_f.

Our data thus indicate that the incorporation of cholesterol reduces the steric pressure, P_s, between EPC bilayers but has little effect on the total pressure, P_t, for applied pressures and fluid separations where steric hindrance is negligible ($\ln P < 17$). These data provide the magnitude and distance dependence of P_t but do not provide direct information on the relative magnitudes of the component pressures, P_s, P_h, P_f, and P_v. The separation of P_t into its components is a formidable task, and a unique solution of the problem is not obtainable at present, partly because the underlying physical bases of these pressures are not completely understood and the X-ray data are at limited resolution. However, on the basis of (1) measurements of the energy of adhesion (Evans & Metcalfe, 1984; Needham, personal communication), (2) recent theoretical treatments for the relationship between P_h and P_f (Evans & Parsegian, 1986; Evans & Needham, 1987), and (3) our previous analysis of P_s (McIntosh et al., 1987), we have modeled the data in Figure 5 in terms of the component pressures. For these modeling calculations we used the following functional forms for each pressure: $P_h(d_0) = P_{h0} \exp(-d_0/\lambda_h)$, $P_s(d_0) = P_{s0} \exp(-d_0/\lambda_s)$, $P_f(d_0) = P_{f0} \exp(-d_0/2\lambda_h)$, and $P_v = -H/6\pi d_0^3$,

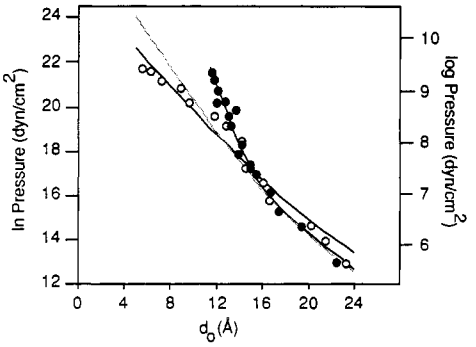

FIGURE 6: Natural logarithm (left-hand scale) and common logarithm (right-hand scale) of aplied pressure plotted versus the distance between the planes or origin (d_0) of P_h, P_f, P_s, and P_v for EPC (solid circles) and equimolar EPC/cholesterol (open circles) bilayers. The solid lines represent least-squares fit to the data points with functional forms for each component pressure as described in the text. The stippled line represents the fit to the equimolar EPC/cholesterol data using magnitudes for P_h and P_f based on the predictions of Simon et al. (1988), Evans and Parsegian (1986), and Evans and Needham (1987). See text for details.

where d_0 is the distance between the planes of origin of each of these interactions. Recent theoretical analyses (Evans & Parsegian, 1986; Evans & Needham, 1987) show that P_{f0} can be expressed in terms of P_{h0}, that is, $P_{f0} = (\pi kT/32\lambda_h)(P_{h0}/B\lambda_h)^{1/2}$, where B is the bilayer bending modulus. The Hamaker constant, H, can be estimated from measured energies of adhesion (see below). Thus, for these four component pressures, there are four independent variables: P_{h0}, λ_h, P_{s0}, and λ_s. As noted by Evans and Parsegian (1986), the planes of origin may differ among these interactions, and there is no clear definition for any of these planes. Following their lead, we also assume that all pressures are measured relative to the same zero separation. We define d_0 from electron density profiles as the distance between head-group peaks from adjacent bilayers. This definition gives values of d_0 that are quite similar to those given by a "mass-average" or Luzzati definition (Luzzati, 1968) of fluid separation used by Evans and Parsegian (1986); Janiak et al. (1979) have shown that the distance between head-group peaks in electron density maps and the Luzzati values for fluid separations are within 2 Å for a wide range of water contents for DMPC bilayers. Our definitions for the distance between the planes of origin of the pressures (d_0) and the distance between bilayer surfaces (d_f) differ by 10 Å, or the approximate width of the EPC head group. Note that d_f was used in the calculations and discussion of steric interactions since it seems easier to understand P_s and the interpenetration of head groups from adjacent bilayers in terms of an origin at the bilayer surface.

For the case of EPC, our procedure was to fit the total pressure curves in Figure 5, using the functional forms for P_h, P_f, P_s, and P_v given above. A value for the Hamaker constant, H, was determined that gave a match between the calculated energy of adhesion and the experimentally measured value of −0.015 erg/cm^2 (Evans & Metcalfe, 1984). The calculated adhesion energy was obtained by intergrating the total pressure and evaluating at the equilibrium fluid spacing. For EPC bilayers, the bending modulus B was set equal to 10^{-12} erg (Servuss et al., 1978; Lorenzen et al., 1986). Using standard statistical methods (Neter & Wasserman, 1974), we obtain the least-squares fit ($r^2 = 0.985$) to the EPC pressure data as shown in Figure 6. The parameters obtained are $P_{h0} = 5.6 \times 10^{11}$ dyn/cm^2, $P_{f0} = 1.8 \times 10^9$ dyn/cm^2, $P_{s0} = 1.1 \times 10^{17}$ dyn/cm^2, $\lambda_h = 1.38$ Å, $\lambda_s = 0.68$ Å, with $H = 2.5 \times 10^{-14}$ erg. Several points should be noted concerning these calculations. First, for EPC bilayers P_s is the dominant repulsive pressure for $d_0 < 15$ Å, whereas P_f is the largest repulsive pressure for $d_0 > 15$ Å. That is, the use of the formalism described above predicts that the interactions between EPC bilayers are dominated by steric and fluctuation pressures, with the hydration pressure of secondary importance. However, excellent fits to the pressure–fluid spacing data can also be obtained without including the P_f term, and by only using P_s and P_h [for example, see Figure 4A of McIntosh et al. (1987)]. Without the inclusion of the P_f term, λ_h is higher by several tenths of an angstrom as shown previously (Evans & Parsegian, 1986; McIntosh et al., 1987). It should also be noted that the value of λ_h is sensitive to changes in bilayer thickness caused by partial dehydration (McIntosh & Simon, 1986a). Small changes in d_b (below 1–2 Å) are not accurately measured in the limited-resolution electron density profiles. However, in large EPC vesicles, aspirated under tensions corresponding to ln $P = 17$, area changes have been observed (Kwok & Evans, 1981) which would correspond to increases in bilayer thickness of between 1 and 2 Å (Simon et al., 1988). Reduction of the values of d_0 to take into account this bilayer deformability can be done by the methods we have used previously (Simon et al., 1988). This procedure increases λ_h to about 1.5 Å when P_f is included and about 2.0 Å when P_f is not included (Simon et al., 1988).

For EPC containing equimolar cholesterol, there was no upward break in the plot of ln P versus fluid spacing (see above and Figure 5). Therefore, we set P_s equal to 0 in this analysis. To determine H, we used an energy of adhesion of −0.02 erg/cm^2, which was measured for equimolar 1-stearoyl-2-oleoylphosphatidylcholine (SOPC)/cholesterol bilayers (David Needham, personal communication). Since EPC has, on the average, a similar hydrocarbon chain composition to SOPC, we assume that the energy of adhesion is similar for EPC/cholesterol and SOPC/cholesterol bilayers. The bilayer bending modulus, B, is proportional to the square of the bilayer hydrocarbon thickness times the bilayer compressibility modulus. Using the electron density profiles (Figure 3) to estimate the hydrocarbon thickness (McIntosh & Simon, 1986b) and published values of the compressibility moduli for SOPC and SOPC/cholesterol bilayers (Evans & Needham, 1987), we estimate that the incorporation of cholesterol increases B by a factor of 6.1. The least-squares fit ($r^2 = 0.965$) to the equimolar EPC/cholesterol data (Figure 6) has $P_{h0} = 8.2 \times 10^{10}$ dyn/cm^2, $P_{f0} = 1.8 \times 10^8$ dyn/cm^2, and $\lambda_h = 1.89$ Å, with $H = 3.6 \times 10^{-14}$ erg. These calculations indicate that the incorporation of cholesterol decreases both P_{h0} and P_{f0}, increases λ_h, and increases H. Several observations can be made concerning the results of these calculations. First, for equimolar EPC/cholesterol P_h is larger than P_f for the range 0 Å $< d_0 <$ 19.6 Å. That is, although P_f may be larger than P_h for EPC bilayers, P_h is the dominant repulsive interaction for a wide range of d_0 when equimolar cholesterol is added to the bilayer. Second, the increase in H would be expected on the basis of cholesterol's increasing the electron density of the bilayer hydrocarbon region (Nir, 1976). Third, for the EPC/cholesterol data, no correction was considered necessary to account for bilayer deformation on the basis of compressibility moduli data. Evans and Needham (1987) measured compressibility moduli of 200 and 1077 dyn/cm for bilayers of SOPC and equimolar SOPC/cholesterol, respectively. This means that the area per molecule and thickness changes for SOPC/cholesterol bilayers are less than 20% as large as for SOPC bilayers. This implies that the change in bilayer thickness for EPC/cholesterol bilayers for applied pressures up to ln $P = 17$ is expected to be less than 0.4 Å.

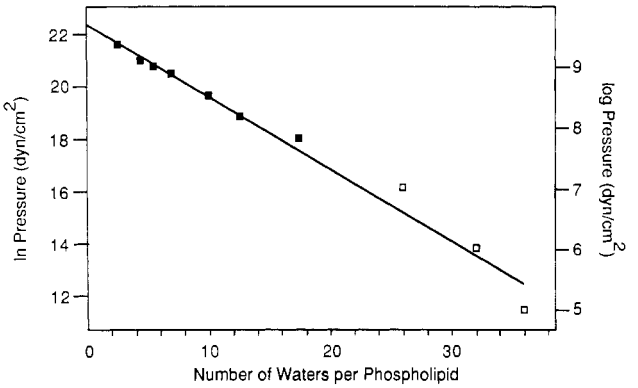

FIGURE 7: Natural logarithm (left-hand scale) and common logarithm (right-hand scale) of applied pressure plotted versus the number of water molecules per EPC molecule. Data were taken from Jendrasiak and Hasty (1974) (solid squares) and Lis et al. (1982) (open squares).

We also used the EPC and EPC/cholesterol data in another way, to explicitly test recent analyses of P_h (Cevc & Marsh, 1985; Simon et al., 1988). In this procedure, we took the best fit to the EPC data (Figure 6) and multiplied P_{h0} by the ratio of the square of dipole potentials for EPC in the presence and absence of cholesterol. That is, the formalism of Cevc and Marsh (1985) showed that P_{h0} is proportional to the square of the bilayer hydration potential, and Simon et al. (1988) found experimentally that the dipole potential, as measured in monolayers, provides a reasonable estimate for the hydration potential. The measured ratio of the square of dipole potentials for equimolar EPC/cholesterol and EPC is (493 mV/415 mV)^2 = 1.4. Thus, the Simon et al. (1988) analysis predicts that P_{h0} should increase by a factor of 1.4 upon the incorporation of equimolar cholesterol. Since ln 1.4 = 0.34, this would not appear as a significant change in plots of ln P versus fluid spacing. With the use of this predicted value for P_{h0}, the fit (r^2 = 0.919) to the EPC/cholesterol data, shown as a stippled line in Figure 6, gives λ_h = 1.42 Å, which is significantly lower than the value of 1.89 Å obtained in the calculation where P_{h0} was varied but is close to the value of 1.38 Å calculated for EPC (see above). (This again illustrates that λ_h is quite sensitive to the assumptions made about the relative magnitudes of P_{h0} and P_{f0}). This fit to the data (Figure 6, stippled line) is not quite as good as that obtained when P_{h0} was varied (Figure 6, solid line). In particular, the values of d_0 at the higher pressures tend to level off and deviate from the stippled line. The theory of Cevc and Marsh (1985) predicts such a behavior at low values of d_0. Thus, taking into account this theory and the experimental uncertainty in the data, we consider that both calculations (solid and stippled lines, Figure 6) match the data points reasonably well. That is, these calculations indicate that the recent theoretical treatments for the magnitude of P_h (Cevc & Marsh, 1985; Simon et al., 1988) and P_f (Evans & Parsegian, 1986; Evans & Needham, 1987) yield predictions that are in reasonably good agreement with the equimolar EPC/cholesterol data.

Independent of the manner in which P_t is separated into its components, the total work to remove water from between adjacent bilayers can be calculated from published data, giving the number of water molecules per lipid molecule for a given applied pressure. The gravimetric measurements of Lis et al. (1982) along with the water sorption measurements of Jendrasiak and Hasty (1974) provide this information (Figure 7) for equimolar EPC/cholesterol bilayers for the pressure range covered by our X-ray experiments. Note that this plot (Figure 7) is approximately linear over the entire pressure range and, in particular, has no break where the head groups from apposing bilayers interpenetrate (at ln $P \cong 20$). This implies that the work to remove water is a continuous process, even as the apposing polar head groups interpenetrate. The work to remove water between the EPC/cholesterol bilayers can be calculated by intergrating under this curve. The energy to dehydrate the bilayers from 34.4 to 2.4 water molecules per EPC molecule is 60 or 66 erg/cm^2, depending on whether an area per molecule of 96 Å^2 (Lis et al., 1982) or 88 Å^2 (Lecuyer & Dervichian, 1969) is used in the calculation. A value of about 88 erg/cm^2 is obtained by integrating the pressure versus d_0 relationship (Figure 6) over an equivalent pressure range. These numbers can be compared to the measured adhesion energy (the energy to bring the bilayers to their equilibrium separation in excess water) of about −0.02 erg/cm^2. Thus, the energy to bring EPC/cholesterol bilayers into a position where the polar layers interpenetrate is about 3500 times the energy of adhesion.

Although cholesterol's ability to increase the area per PC head group appears to be the key to reducing steric repulsion, the plots of ln P versus d_f for ln $P < 17$ (Figure 5) and our dipole potential measurements indicate that, in terms of the hydration pressure, cholesterol is doing more than acting as a "spacer" molecule in the membrane. That is, if cholesterol's only effect were to spread the EPC head groups apart in the plane of the membrane, then cholesterol would be expected to decrease the bilayer dipole potential and significantly reduce P_h. For example, MacDonald and Simon (1987) have found for monolayers of dimyristoylphosphatidylcholine that the dipole potential is inversely proportional to the area per lipid molecule, and we (Simon et al., 1988) have found for the gel, liquid-crystalline, and interdigitated lamellar phases of PC that P_h decreases with increasing area per molecule. Thus, since the incorporation of cholesterol increases the area per EPC head group but increases dipole potential, cholesterol must be reorganizing interfacial water, as well as separating the lipid head groups.

The analysis presented above concerning cholesterol's ability to reduce the steric hindrance of the PC head group may have implications in terms of the close approach of both adjacent bilayers and small hydrophobic molecules. For instance, in studies of divalent cation mediated fusion of lipid vesicles it has been found that PC and other choline-containing lipids have an inhibitory effect on vesicle association (Stamatatos & Silvius, 1987). However, when a high concentration of cholesterol (equimolar PC/cholesterol) is added to the vesicles, this inhibitory effect of the PC head groups is diminished (Stamatatos & Silvius, 1987). This may be due in part to cholesterol's ability to spread apart the PC head groups and reduce the steric repulsion between adjacent bilayers. For charged vesicles, the incorporation of cholesterol would increase the magnitude of the adhesion energy by reducing the density of charged head groups in the plane of the bilayer. In the case of small molecules, the incorporation of equimolar concentrations of cholesterol into bilayers would increase the accessibility to the hydrocarbon–water interface for molecules with diameters smaller than a PC head group (i.e., most metabolites). That is, with cholesterol in the bilayer, these small molecules could gain access to the interface without exerting the work necessary to enter and distort the polar head-group region of the bilayer.

ACKNOWLEDGMENTS

We thank Dr. Michael Hines for his expert assistance in the computer curve fitting.

Registry No. Cholesterol, 57-88-5.

REFERENCES
Attard, P., Mitchell, D. J., & Ninham, B. W. (1988) *Biophys. J. 53*, 457–460.
Blaurock, A. E., & Worthington, C. R. (1966) *Biophys. J. 9*, 305–312.
Cevc, G., & Marsh, D. (1985) *Biophys. J. 47*, 21–32.
Cohen, B. Z. (1975) *J. Membr. Biol. 20*, 205–234.
Darke, A., Finer, E. G., Flook, A. G., & Phillips, M. C. (1972) *J. Mol. Biol. 63*, 265–279.
Evans, E., & Metcalfe, M. (1984) *Biophys. J. 46*, 423–426.
Evans, E. A., & Parsegian, V. A. (1986) *Proc. Natl. Acad. Sci. U.S.A. 83*, 7132–7136.
Evans, E., & Needham, D. (1987) *J. Phys. Chem. 91*, 4219–4228.
Franks, N. P. (1976) *J. Mol. Biol. 100*, 345–358.
Franks, N. P., & Lieb, W. R. (1979) *J. Mol. Biol. 133*, 469–500.
Harbich, W., & Helfrich, W. (1984) *Chem. Phys. Lipids 36*, 39–63.
Hauser, H., Pascher, I., Pearson, R. H., & Sundell, S. (1981) *Biochim. Biophys. Acta 650*, 21–51.
Haydon, D. A., & Hladky, S. B. (1972) *Q. Rev. Biophys. 5*, 187–282.
Herbette, L., Marquardt, J., Scarpa, A., & Blasie, J. K. (1977) *Biophys. J. 20*, 245–272.
Israelachvili, J. N., & Pashley, R. M. (1983) *Nature (London) 306*, 249–250.
Janiak, M. J., Small, D. M., & Shipley, G. G. (1979) *J. Biol. Chem. 254*, 6068–6078.
Jendrasiak, G. L., & Hasty, J. H. (1974) *Biochim. Biophys. Acta 337*, 79–91.
King, G. I., & Worthington, C. R. (1971) *Phys. Lett. A. 35A*, 259.
Kwok, R., & Evans, E. (1981) *Biophys. J. 35*, 637–652.
Lecuyer, H., & Dervichian, D. G. (1969) *J. Mol. Biol. 45*, 39–57.
LeNeveu, D. M., Rand, R. P., & Parsegian, V. A. (1976) *Nature (London) 259*, 601–603.
LeNeveu, D. M., Rand, R. P., Parsegian, V. A., & Gingell, D. (1977) *Biophys. J. 18*, 209–230.
Lesslauer, W., Cain, J. E., & Blasie, J. K. (1972) *Proc. Natl. Acad. Sci. U.S.A. 69*, 1499–1503.
Lis, L. J., McAlister, M., Fuller, N., Rand, R. P., & Parsegian, V. A. (1982) *Biophys. J. 37*, 657–666.
Lorenzen, S., Servuss, R. M., & Helfrich, W. (1986) *Biophys. J. 50*, 565–572.
Luzzati, V. (1968) in *Biological Membranes* (Chapman, D., Ed.) pp 71–123, Academic, New York.
MacDonald, R. C., & Simon, S. A. (1987) *Proc. Natl. Acad. Sci. U.S.A. 84*, 4089–4094.
Marcelja, S., & Radic, N. (1976) *Chem. Phys. Lett. 42*, 129–130.
McIntosh, T. J. (1978) *Biochim. Biophys. Acta 513*, 43–58.
McIntosh, T. J. (1980) *Biophys. J. 29*, 237–246.
McIntosh, T. J., & Simon, S. A. (1986a) *Biochemistry 25*, 4058–4066.
McIntosh, T. J., & Simon, S. A. (1986b) *Biochemistry 25*, 4948–4952.
McIntosh, T. J., Magid, A. D., & Simon, S. A. (1987) *Biochemistry 26*, 7325–7332.
Neter, J., & Wasserman, W. (1974) *Applied Linear Statistical Methods*, p 228, R. D. Irwin, Inc., Homewood, Illinois.
Nir, S. (1976) *Prog. Surf. Sci. 8*, 1–58.
O'Brien, F. E. M. (1948) *J. Sci. Instrum. 25*, 73–76.
Oldfield, E., & Chapman, D. (1972) *FEBS Lett. 21*, 303–306.
Parsegian, V. A., Fuller, N., & Rand, R. P. (1979) *Proc. Natl. Acad. Sci. U.S.A. 76*, 2750–2754.
Parsegian, V. A., Rand, R. P., Fuller, N. L., & Rau, R. C. (1986) *Methods Enzymol. 127*, 400–416.
Pearson, R. H., & Pascher, I. (1979) *Nature (London) 281*, 499–501.
Servuss, R. M., Harbich, W., & Helfrich, W. (1978) *Biochim. Biophys. Acta 436*, 900–903.
Shannon, C. E. (1949) *Proc. Inst. Radio Eng. N.Y. 37*, 10–21.
Simon, S. A., McIntosh, T. J. & Latorre, R. (1982) *Science (Washington, D.C.) 216*, 65–67.
Simon, S. A., McIntosh, T. J. & Magid, A. D. (1988) *J. Colloid Interface Sci.* (in press).
Small, D. M., & Shipley, G. G. (1974) *Science (Washington D.C.) 185*, 222–229.
Stamatatos, L., & Silvius, J. R. (1987) *Biochim. Biophys. Acta 905*, 81–90.
Stockton, G. W., & Smith, I. C. P. (1976) *Chem. Phys. Lipids 17*, 251–263.
Szabo, G. (1974) *Nature (London) 252*, 47–49.
Szabo, G. (1976) in *Membrane Toxicity* (Miller, M. W., & Shamoo, A. E., Eds.) pp 167–190, Plenum, New York.
Tardieu, A., Luzzati, V., & Reman, F. C. (1973) *J. Mol. Biol. 75*, 711–733.
Taylor, R. P., Huang, C., Broccoli, A. V., & Leake, L. (1977) *Arch. Biochem. Biophys. 183*, 83–89.
Ter-Minassian-Saraga, L., & Madelmont, G. (1982) *FEBS Lett. 137*, 137–141.
Torbet, J., & Wilkins, M. H. F. (1976) *J. Mol. Biol. 62*, 447–458.
Vink, H. (1971) *Eur. Polymer J. 7*, 1411–1419.
Weast, R. C. (1984) *Handbook of Chemistry and Physics*, 65th ed., p E-42, CRC Press, Boca Raton, FL.
Worcester, D. L., & Franks, N. P. (1976) *J. Mol. Biol. 100*, 359–378.